doi:10.1093/brain/awz022 BRAIN 2019: 142; 978–991 | 978

BRAIN
A JOURNAL OF NEUROLOGY

A year-long immune profile of the systemic response in acute stroke survivors

Amy S. Tsai,[1] Kacey Berry,[2,3] Maxime M. Beneyto,[1] Dyani Gaudilliere,[4] Edward A. Ganio,[1] Anthony Culos,[1] Mohammad S. Ghaemi,[1] Benjamin Choisy,[1] Karim Djebali,[1] Jakob F. Einhaus,[1] Basile Bertrand,[1] Athena Tanada,[1] Natalie Stanley,[1] Ramin Fallahzadeh,[1] Quentin Baca,[1] Lisa N. Quach,[2,3] Elizabeth Osborn,[2,3] Lauren Drag,[3] Maarten G. Lansberg,[2,3] Martin S. Angst,[1] Brice Gaudilliere,[1,*] Marion S. Buckwalter[2,3,5,*] and Nima Aghaeepour[1,*]

*These authors contributed equally to this work.

Stroke is a leading cause of cognitive impairment and dementia, but the mechanisms that underlie post-stroke cognitive decline are not well understood. Stroke produces profound local and systemic immune responses that engage all major innate and adaptive immune compartments. However, whether the systemic immune response to stroke contributes to long-term disability remains ill-defined. We used a single-cell mass cytometry approach to comprehensively and functionally characterize the systemic immune response to stroke in longitudinal blood samples from 24 patients over the course of 1 year and correlated the immune response with changes in cognitive functioning between 90 and 365 days post-stroke. Using elastic net regularized regression modelling, we identified key elements of a robust and prolonged systemic immune response to ischaemic stroke that occurs in three phases: an acute phase (Day 2) characterized by increased signal transducer and activator of transcription 3 (STAT3) signalling responses in innate immune cell types, an intermediate phase (Day 5) characterized by increased cAMP response element-binding protein (CREB) signalling responses in adaptive immune cell types, and a late phase (Day 90) by persistent elevation of neutrophils, and immunoglobulin M^+ (IgM^+) B cells. By Day 365 there was no detectable difference between these samples and those from an age- and gender-matched patient cohort without stroke. When regressed against the change in the Montreal Cognitive Assessment scores between Days 90 and 365 after stroke, the acute inflammatory phase Elastic Net model correlated with post-stroke cognitive trajectories ($r = -0.692$, Bonferroni-corrected $P = 0.039$). The results demonstrate the utility of a deep immune profiling approach with mass cytometry for the identification of clinically relevant immune correlates of long-term cognitive trajectories.

1 Department of Anesthesiology, Perioperative and Pain Medicine, Stanford School of Medicine, 94305 CA, USA
2 Stanford Stroke Center, Stanford School of Medicine, 94305, CA, USA
3 Department of Neurology and Neurological Sciences, Stanford School of Medicine, 94305 CA, USA
4 Division of Plastic and Reconstructive Surgery, Department of Surgery, Stanford School of Medicine, 94305 CA, USA
5 Department of Neurosurgery, Stanford School of Medicine, 94305 CA, USA

Correspondence to: Brice Gaudilliere
Department of Anesthesiology, Perioperative and Pain Medicine, 300 Pasteur Drive, Room S238, Stanford, CA 94305-5117, USA
E-mail: gbrice@stanford.edu

Received August 11, 2018. Revised November 18, 2018. Accepted December 14, 2018. Advance Access publication March 12, 2019

Correspondence may also be addressed to: Marion S. Buckwalter
Stanford Stroke Center, Department of Neurology, Department of Neurosurgery, 1201 Welch Rd
Room P209, Stanford, CA 94305-5117, USA
E-mail: marion.buckwalter@stanford.edu

Nima Aghaeepour
Department of Anesthesiology, Perioperative and Pain Medicine
300 Pasteur Drive, Room S238, Stanford, CA 94305-5117, USA
E-mail: naghaeep@stanford.edu

Keywords: stroke; cognitive outcomes; systemic immunology; mass cytometry; machine learning

Abbreviations: CREB = cAMP response element-binding protein; M-MDSCs = monocytic-myeloid-derived suppressor cells; MoCA = Montreal Cognitive Assessment; STAT = signal transducer and activator of transcription

Introduction

After suffering a stroke, a patient's cognitive and functional trajectory is complex. Cognitive outcomes vary widely between patients, even for those who suffer similar acute deficits, and initial recovery can be followed by later insidious declines (Ivan *et al.*, 2004; Levine *et al.*, 2015; Corraini *et al.*, 2017; Dhamoon *et al.*, 2017). Because the biological mechanisms of recovery from stroke remain poorly understood, therapeutic interventions to improve outcomes are lacking. Identifying a set of post-stroke biomarkers that predicts functional and cognitive outcomes after stroke would provide a powerful step forward. These biomarkers could help identify patients at the greatest risk for impaired recovery or delayed-onset decline and furthermore, could set a foundation for understanding the biological mechanisms that underlie outcome trajectories. Both will be critical for future endeavours aimed at improving recovery from stroke and preventing post-stroke cognitive decline/dementia.

Peripheral blood immune cells and secreted inflammatory mediators provide a promising and easily accessible biological substrate to search for such biomarkers and understand the mechanistic underpinnings of stroke recovery. Stroke induces an acute immune response that engages both local and peripheral immunological compartments. Previous studies in humans (Mena *et al.*, 2004; Doyle *et al.*, 2015) and rodent models (Jin *et al.*, 2010) have predominantly focused on the local and short-term (hours to days) immune response to stroke. These studies have demonstrated that in the first few days after stroke, resident brain cells (astrocytes and microglia) and invading innate immune cells (primarily neutrophils and monocytes) are implicated in mechanisms that determine stroke outcomes weeks to months later (Iadecola and Anrather, 2011). Additionally, chronic adaptive immune responses detectable in the stroke core cause delayed cognitive impairment after stroke in mice, manifesting 7–12 weeks after the infarct (Doyle *et al.*, 2015; Doyle and Buckwalter, 2017). One major concern is the lack of applicability of findings based on rodent models to humans. For example, a recent clinical trial showed that natalizumab failed to reduce infarct volumes despite promising results from studies in animal models (Elkins *et al.*, 2017). Having more data on long- as well as short-term peripheral immune responses in humans may thus be helpful in understanding which animal findings will translate to humans in the future.

Several lines of evidence suggest that immune responses detectable in peripheral blood relate to early innate and later adaptive immune responses in the brain (Fassbender *et al.*, 1997; Becker *et al.*, 2005; Mayer *et al.*, 2013; Chamorro *et al.*, 2016). Numerous studies have focused on circulating plasma cytokines and the distribution of peripheral immune cells after stroke (Kim *et al.*, 1996; Bustamante *et al.*, 2016). Although modest correlates of clinical recovery after stroke were reported—notably an association between interleukin (IL)-6 plasma levels early after stroke and worse clinical outcomes (Kim *et al.*, 1996; Waje-Andreassen *et al.*, 2005)—bulk cytokine responses alone provide little mechanistic insight into the biology that drives recovery. Instead, analysing the specific types of immune cells that are responding to these circulating cytokines and chemokines might provide greater insight into the biological mechanisms of recovery. The advent of single-cell techniques, furthermore, provides an opportunity to investigate these specific immune cell types and their functional attributes with a high level of granularity.

We therefore chose mass cytometry to profile the peripheral immune response to stroke in patients over the course of 1 year. Mass cytometry is a powerful single-cell technology that comprehensively monitors the functional state of the immune system. It merges traditional flow cytometry with inductively-coupled plasma mass spectrometry to assess up to 50 phenotypic and functional parameters on a cell-by-cell basis. As such, mass cytometry allows the simultaneous quantification of multiple attributes in all major immune cell types, including cell phenotype and frequency as well as the activity of key intracellular signalling pathways. The concept of using mass cytometry 'at the bedside' for the deep profiling of immune mechanisms associated with disease pathogenesis has been demonstrated in multiple clinical contexts, including ageing (Mrdjen *et al.*, 2018), malignancies (Wogsland *et al.*, 2017), pregnancy

(Aghaeepour *et al.*, 2017; Ghaemi *et al.*, 2018) and traumatic injury (Gaudillière *et al.*, 2014; Tárnok, 2015).

Here, we combine a deep immune profiling mass cytometry approach with an unbiased elastic net analysis of immune signalling networks to comprehensively and functionally characterize patients' peripheral immune cell responses over a 1-year period after stroke. The primary goal of the study was to determine if mass cytometry could be used to detect and describe the chronology of the peripheral immune response over the course of 1 year after stroke. A secondary goal was to ascertain whether the magnitude of specific immune responses is associated with the long-term cognitive trajectory after stroke.

Materials and methods

Subjects

The study was conducted at Stanford School of Medicine (Stanford, CA, USA) and was approved by Stanford's Institutional Review Board. Informed consent was obtained from patients and their surrogates in person. Twenty-five patients were enrolled within 24 h of stroke onset (patient demographics are listed in Table 1). Serial whole blood samples were collected at up to nine time points over the course of 1 year following stroke (Days 1, 2, 3, 5, 7, 14, 30, 90, and 365). Recruitment occurred between March 2015 and June 2016. Enrolled patients met the inclusion criteria: age 18 or older, acute stroke as diagnosed by Stanford neurologists based on clinical assessment and confirmation of acute infarction on CT or MRI imaging, ability to sign informed consent, ability to return for follow-up visits, and ability to undergo serial blood draws and cognitive assessment. Exclusion criteria were a history of autoimmune disorder, use of immunosuppressant drugs within 6 months prior to the study, and life expectancy <90 days. One subject died prior to the 1-day time point and was not included in the mass cytometry study. Of the five subjects in the study who did not complete the 1-year time point, one died, one was lost to follow-up, two refused blood draws, and one moved out of the country and was unable to return for follow-up. Screening logs were not kept for this study, but patients were recruited sequentially according to clinical coordinator availability for consent and blood draws.

A separate healthy cohort of 24 sex- and age-matched controls undergoing hip replacement surgery was also included to allow comparing the magnitude of immunological change observed in response to ischaemic brain injury and in response to traumatic injury. Banked samples from the surgical cohort were analysed for this study (Supplementary Table 1).

Cognitive testing

A cognitive battery that included the Montreal Cognitive Assessment (MoCA), a 30-item cognitive screen, was administered on Days 3, 30, 90 and 365. Subjects were excluded from the cognitive testing if they did not speak English as a primary language or if they exhibited significant aphasia, delirium, blindness, or other factors that limited their ability to participate in the cognitive assessment. Three alternate forms of the MoCA were administered across time points to prevent learning effects (Day 3, version 2; Day 30, version 1; Day 90, version 3; Day 365, version 2). Cognitive improvement or stability was classified as positive or no change in MoCA scores from Days 90 to 365, while decline was classified as a negative change.

Subjects were given hard copy surveys of the Center for Epidemiological Studies-Depression (CES-D) and fatigue questionnaires to fill out. The CES-D scale is a validated self-report questionnaire intended to detect symptoms and severity of depression in the general population (Radloff, 1977). Research technicians provided reading or writing assistance as needed. In the event that subjects were unable to complete these questionnaires due to receptive aphasia, close family members were asked to provide answers. We used the short-form Neuro-QOL Fatigue Scale to assess current levels of fatigue (Cella *et al.*, 2012). This brief 8-item self-report measure uses a Likert rating scale. Scores range from 8 to 40 with higher scores indicating higher levels of fatigue.

Determination of stroke size and location

Stroke volumes and locations were assessed by a reader blinded to the immunological data on the diffusion-weighted sequence of a clinical MRI scan obtained during hospital admission for index stroke. If an MRI was not obtained, the infarct was assessed on non-contrast CT instead ($n = 3$). Lesions were manually outlined using the polygon region of interest tool in Osirix software (version 8.0), and total infarct volumes were calculated based on these outlines in Osirix. Lesions <1 cm^3 were assigned a volume of 1 cm^3 for the statistical analyses.

Sample collection and whole blood processing

Whole blood was collected in 10 ml heparin-containing tubes at several time points over the course of 1 year, with at least two and up to eight time points per patient (Fig. 1A and B). Within 30 min of collection, samples were divided into 1 ml aliquots (Smart Tube, Inc.). Samples were stored at -80°C until further processing. The processing protocol for mass cytometry analysis was similar to that of previous clinical studies (Gaudillière *et al.*, 2014).

Erythrocyte lysis

Fixed samples were thawed for 30 min on ice and then for 15 min at room temperature. Samples were then filtered using a 100 µm membrane into a hypotonic erythrocyte lysis buffer (Smart Tube, Inc.) and incubated for 10 min at room temperature. Samples were centrifuged to pellet leucocytes, and the supernatant was removed. Samples were resuspended in the lysis buffer for an additional 5 min, then centrifuged again to obtain a leucocyte pellet for subsequent processing.

Sample barcoding

After erythrocyte lysis, leucocytes were barcoded as previously described (Behbehani *et al.*, 2014). In summary, cells were

Table 1 Population and clinical characteristics of stroke cohort

Demographics	
Age, years, mean ± SD [median (min–max)]	63.3 ± 17.4 [65.5 (24.0–88.0)]
Female sex, *n* (%)	10 (41.7)
Body mass index, kg/m^2, mean ± SD	29.1 ± 7.3
Race, *n* (%)	
White (Europe, Middle East, North Africa)	17 (70.8)
Asian [Far East, Southeast Asia, or the Indian subcontinent (includes Philippine Islands)]	3 (12.5)
Black or African American	0 (0.0)
Other (American Indian, Alaskan Native, Central/South American, Native Hawaiian or other Pacific Islander)	4 (16.7)
Ethnicity, *n* (% Hispanic, Latino or Spanish origin)	4 (16.7)
Stroke parameters	
Stroke size, median, cm^3 (min–max)	7.75 (1–102)
Acute treatments, *n* (%)	
IV-tPA)	5 (20.8)
Intra-arterial therapy (IAT)	1 (4.2)
IAT and IV-tPA	8 (33.3)
Location[a], *n* (%)	
Right hemisphere lesion	16 (66.7)
Brainstem	0 (0.0)
Caudate	9 (37.5)
Cerebellum	3 (12.5)
Frontal	5 (20.8)
Insula	6 (25.0)
Lentiform	5 (20.8)
Occipital	1 (4.2)
Parietal	5 (20.8)
Temporal	8 (33.3)
Thalamus	1 (4.2)
Left hemisphere lesion	9 (37.5)
Brainstem	1 (4.2)
Caudate	0 (0.0)
Cerebellum	1 (4.2)
Frontal	2 (8.3)
Insula	2 (8.3)
Lentiform	0 (0.0)
Occipital	1 (4.2)
Parietal	2 (8.3)
Temporal	0 (0.0)
Thalamus	3 (12.5)
Comorbidities, *n* (%)	
Arterial hypertension	16 (66.7)
Diabetes mellitus	4 (16.7)
Atrial fibrillation	4 (16.7)
Hyperlipidaemia	6 (25.0)
Coronary artery disease	2 (8.3)
Tobacco use	3 (12.5)
Outcome measures	
MoCA score at 1 year post-stroke, median (min–max)	26.5 (16–30)
NIHSS, median (min–max)	
Day 1	2 (0–20)
Day 90	0 (0–11)
Day 365	0 (0–10)

[a]One patient had bilateral lesions, which were separated here.
IV-tPA = intravenous tissue plasminogen activator.

transferred to a 2 ml deep-well block and washed once with Cell Staining Media [phosphate-buffered saline (PBS) supplemented with 0.5% bovine serum albumin (BSA) and 0.02% NaN_3], once with PBS, and once with 0.02% saponin in PBS. Barcode plates, prepared with 20 unique combinations of three of six Pd isotopes (^{102}Pd, ^{104}Pd, ^{105}Pd, ^{106}Pd, ^{108}Pd, or ^{110}Pd),

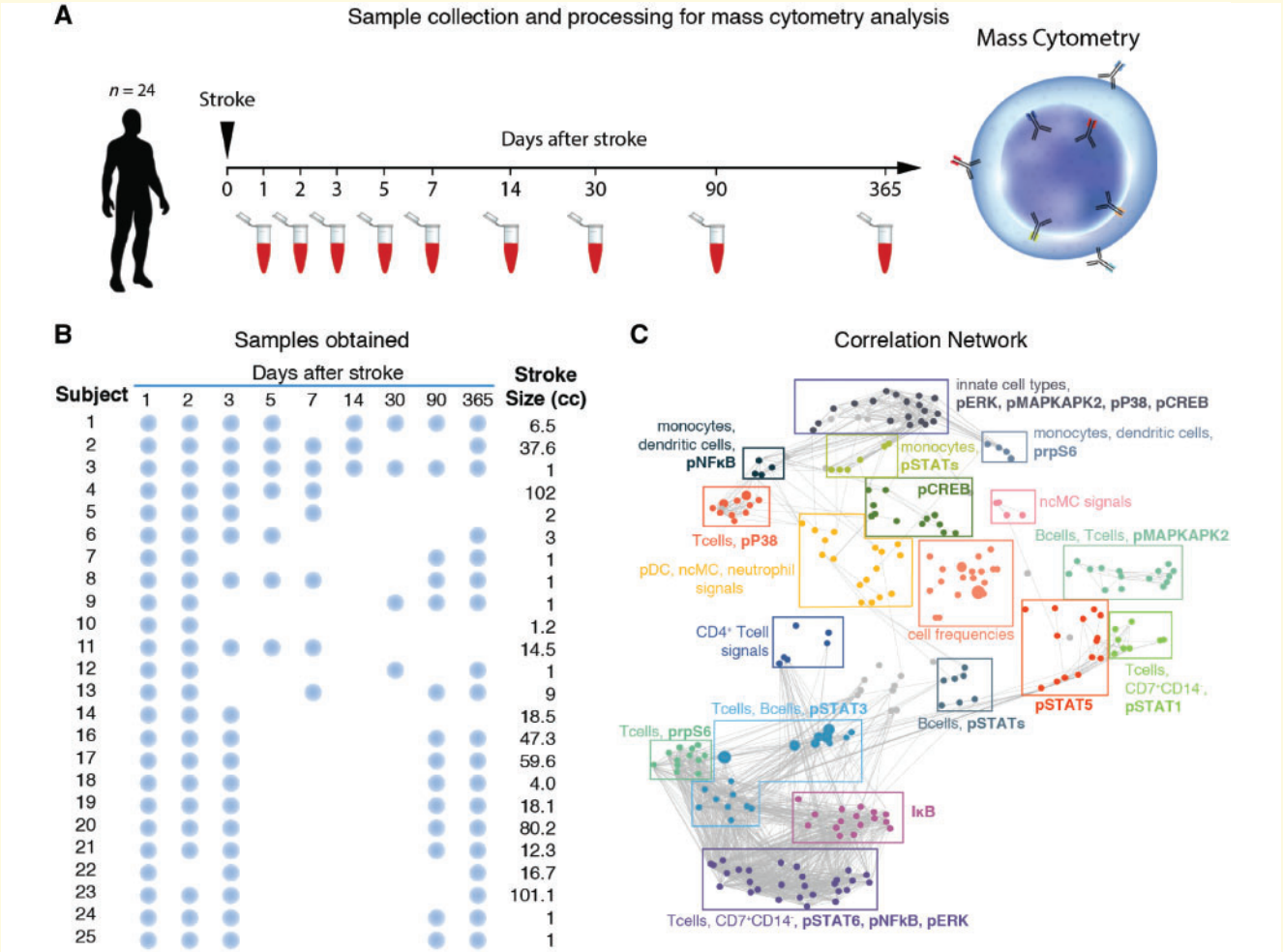

Figure 1 Experimental workflow and predictive modelling. (**A**) Twenty-four patients with acute ischaemic stroke participated in the study. A whole blood sample was obtained at up to nine time points (1, 2, 3, 5, 7, 14, 30, 90, and 365 days) following stroke onset. Samples were processed and analysed using mass cytometry (CyTOF). (**B**) Representation of blood collection from each of the 24 enrolled subjects. Blue dots indicate days on which blood was obtained for each subject. (**C**) The mass cytometry data formed a correlation network that visually segregated into 18 communities containing inter-correlated immune features that changed together during the stroke recovery process. Clusters were annotated based on immune feature attributes (cell subset, signalling property or frequency) that were most commonly represented within each community. pDC = plasmacytoid dendritic cells; ncMCs = $CD14^{-}CD16^{+}$ non-classical monocytes.

were thawed and diluted in 1 ml of 0.02% saponin in PBS (Zunder *et al.*, 2015). Diluted barcode reagents were transferred to each of 20 separate leucocyte samples per preparation. Leucocytes were incubated with barcoding reagents at room temperature for 15 min, washed twice with cell staining media, then pooled for antibody staining. All samples collected from each patient were barcoded and pooled in the same preparation with a gender- and age-matched healthy control (Supplementary Table 1).

Antibody staining

In addition to barcode and iridium-based DNA markers, the panel included 27 antibodies for the phenotyping of all major immune cell subsets and 11 antibodies for the functional characterization of each immune cell (Supplementary Table 2). Antibodies were either obtained pre-conjugated (Fluidigm, Inc.) or were obtained as purified, carrier-free (no BSA or gelatin) versions, which were then conjugated in-house with trivalent metal isotopes using the MaxPAR antibody conjugation kit (Fluidigm, Inc.).

Pooled barcoded cells were washed with cell staining media before being incubated with Fc block (BioLegend) for 10 min at room temperature. Cells were stained with phenotypic (surface) marker antibodies for 30 min with gentle shaking at room temperature. Cells were washed twice with cell staining media and permeabilized with 700 µl of 100% methanol for 10 min at 4°C. Cells were washed twice with PBS, once with cell staining media, and then stained with functional (intracellular) marker antibodies for 30 min with gentle shaking at room temperature. Cells were washed twice with cell staining media and incubated at 4°C overnight in PBS containing an iridium-based DNA intercalator (Fluidigm, Inc.) and 1.5% paraformaldehyde (Electron Microscopy Sciences). Cells were washed twice with ultrapure water (Milli-Q, Millipore Corporation), added to an aqueous suspension of

normalization beads (Fluidigm, Inc.), and filtered through a 35 µm membrane prior to mass cytometry analysis.

Mass cytometry

Barcoded and antibody-stained cells were analysed on the Helios mass cytometer (Fluidigm, Inc.) at a rate of 600 to 1000 events per second. The resulting data were normalized using Normalizer v0.1 MATLAB Compiler Runtime (MathWorks) (Finck *et al.*, 2013). Files were then de-barcoded with a single-cell MATLAB debarcoding tool (Zunder *et al.*, 2015). Gating was performed using Cytobank flow cytometry analysis software (Cytobank, Inc.) according to the gating strategy in Supplementary Fig. 1. The following cell types were included in the analysis: neutrophils, B-cells, immunoglobulin (Ig)M$^+$ B-cells, CD4$^+$ naïve T ($T_{naïve}$) cells, CD4$^+$ memory T (T_{mem}) cells, CD8$^+$$T_{naïve}$ cells, CD8$^+$$T_{mem}$ cells, Tbet$^+$CD4$^+$CD45RA$^+$ cells, Tbet$^+$CD4$^+$CD45RA$^-$ Helper T (Th1) cells, Tbet$^+$CD8$^+$CD45RA$^+$T cells, Tbet$^+$CD8$^+$CD45RA$^-$ cells, regulatory T-cells (T_{regs}), CD66$^-$CD3$^-$CD19$^-$CD14$^-$CD7$^+$ [this parent population referred to as CD14$^-$CD7$^+$ cells includes both CD56^{lo}CD16$^+$ and CD56$^+$CD16$^-$ natural killer (NK) cell subpopulations], CD14$^+$CD16$^-$ monocytes, CD16$^+$CD14$^-$ non-classical monocytes, CD14$^+$CD16$^+$ intermediate monocytes, monocytic myeloid-derived suppressor cells (M-MDSCs), myeloid dendritic cells, and plasmacytoid dendritic cells.

Statistical analysis

Using the elastic net regularized regression method, which performs feature selection while creating mathematical models, 36 models that comprehensively compared each of the nine time points to each of the other eight were generated (Zou and Hastie, 2005). Missing data points were not included in elastic net analysis. Signalling responses were quantified as the arcsinh transformed value for elastic net analysis. Univariate *P*-values for individual immune features (frequencies and functional responses) were obtained using a Wilcoxon test. Spearman's correlations for associations between change in (Δ)MoCA, stroke volume, and elastic net model values were determined using SPSS. *P*-values were Bonferroni-corrected for three comparisons (ΔMoCA or stroke volume compared to elastic net model values of each of the three models). Confounding variables were controlled for using linear regression in SPSS.

Based on previous data documenting the activation of STAT3 and MAPK signalling pathways in monocytes subsets (M-MDSCs) 24 h after surgery (Gaudillière *et al.*, 2014) we estimated that a sample size of 24 patients would be sufficient to provide 95% power at $P < 0.05$ to detect a >40% change in STAT3 phosphorylation in monocyte subsets (effect size of 1.96) using student's *t*-statistic, at the 24-h time point. This power analysis was performed using G*Power (Faul *et al.*, 2007). In addition, for exploratory analysis, we excluded the multivariate models which failed to produce statistically significant results on previously unseen patients during cross-validation. This combination of power analysis based on historical data (for study design) and stringent cross-validation once the dataset is available minimizes the risk of false positive discoveries due to small sample size and enables exploratory analysis at key time points with sufficient effect sizes.

Data availability

Raw data are publicly available at http://flowrepository.org under experiment ID FR-FCM-ZYSB. Anonymous access is provided at http://flowrepository.org/id/FR-FCM-ZYSB. Sample annotations are provided in an attachment uploaded to the repository. Extracted features are available at https://nalab.stanford.edu/wp-content/uploads/strokedata.zip.

Results

Study cohort and workflow

Patient characteristics are listed in Table 1. Nineteen of 24 subjects were studied for the entire 1-year post-stroke period. One subject died prior to the Day 90 collection and four subjects were lost to follow-up. A study workflow with comprehensive sample collection is shown in Fig. 1A and B.

Single-cell profiling of the systemic immune response to acute ischaemic stroke

Using a 47-parameter mass cytometry assay (Supplementary Table 2), 240 immune features were measured in 20 peripheral immune cell subtypes representative of both adaptive and innate immunity. Features collected included cell frequencies and the activity of 11 intracellular signalling proteins, including phosphorylated (p) signal transducer and activator of transcription (STAT)1, STAT3, STAT5, STAT6, protein(P)38, extracellular signal-regulated kinases (ERK), Mitogen-activated protein kinase-activated protein kinase 2 (MAPKAPK2), plastid ribosomal protein S6 small ribosomal subunit (S6), cAMP response element-binding protein (CREB), and nuclear factor kappa-light-chain-enhancer of activated B cells (NF-κB), as well as total nuclear factor of Kappa-light-polypeptide-gene-enhancer in B-cells inhibitor (IκB) degradation. These features allow for the functional assessment of canonical cellular signalling responses implicated in the sterile inflammatory response observed in the context of traumatic injury (Gaudillière *et al.*, 2014), as well as ischaemic brain injury (Wang *et al.*, 2007). For instance, danger-associated molecular patterns (DAMPs), such as peroxiredoxin and high mobility group protein B1 (HMGB1), produced by the necrosing brain cells are released, bind to Toll-like receptors (TLRs), and activate key elements of the myeloid differentiation primary response-88 (MyD88, including P38, ERK, MAPKAPK2, S6, CREB) and NF-κB pathways in innate immune cell subsets. Innate immune cells in turn produce proinflammatory cytokines such as IL-6, IL-12,

and IL-23, which promote the survival, proliferation, and recruitment of additional innate and adaptive immune cells, via activation of the JAK/STAT signalling pathways (Konoeda *et al.*, 2010; Shichita *et al.*, 2012; Pavlov *et al.*, 2018). Signalling responses were measured in samples that were minimally perturbed experimentally (i.e. whole blood was processed within 30 min of collection), allowing the assessment of endogenous immune responses close to *in vivo* conditions.

The mass cytometry data formed a network of correlated immune features (cell frequencies or cell-specific immune signalling responses) at each time point, demonstrating the interconnectivity of the immunological dataset (Fig. 1C). The network was visually segregated into 18 communities to highlight the modularity of the mass cytometry data. Communities were described based on the cell types, cell frequency change, or functional attributes that appeared most frequently within each module.

The interconnected and highly modular nature of the data justified the use of an elastic net algorithm to identify short- and long-term systemic immune features that were significantly different between specified time points after acute stroke (Zou and Hastie, 2005; Aghaeepour *et al.*, 2017). To assess how immune responses change over time, we chose the 1-year (Day 365) time point as a reference time point for the elastic net analyses of time-dependent immune responses after stroke, allowing each patient to serve as his/her own internal control, rather than a cross-sectional assessment at each time point. The results showed no differences in these immune features between samples collected at Day 365 following stroke and in pre-surgical samples collected from patients (Supplementary Fig. 2).

An elastic net analysis identifies three distinct inflammatory phases following an acute ischaemic stroke

The high-dimensional immunological dataset generated at each time point was compared to the 1-year dataset using the multivariate elastic net approach. The analysis demonstrated that a common immune response is detectable in peripheral immune cells for at least 3 months following stroke. Three models were selected for further discussion as they passed stringent cross-validation. Each model contains individual features representative of how the immune response to stroke was different at that time point compared to the 1-year time point (Fig. 2). These are non-overlapping immune features representative of three distinct phases of the systemic immune response to stroke: an acute phase emphasizing immune responses occurring at Day 2, an intermediate phase (Day 5), and a late phase (Day 90). The first model was built on 84 features comparing Day 2 to the 1-year time point, and it had a cross-validated *P*-value of 6.02×10^{-5} (Supplementary Table 3). The second model was built on 21 features comparing Day 5 to the 1-year time point and had a cross-validated *P*-value of 0.0125 (Supplementary Table 4). The third model was built on seven features from the Day 90 to the 1-year time point comparison and had a cross-validated *P*-value of 5.67×10^{-9} (Supplementary Table 5).

To provide an estimate of the relative magnitude of the aggregate immunological features represented by each model over time, each elastic net model was projected onto the immunological dataset from all the time points (Fig. 3). Results from these projections demonstrate that the three elastic net models represent acute (Fig. 3B), intermediate (Fig. 3C), and late phase (Fig. 3D) inflammatory responses, as each model peaks around the appropriate time point.

Elastic net model components reveal sequential engagement of innate and adaptive immune cell responses

Taken together, the analysis revealed a chronology of interrelated immune events that characterized three distinct inflammatory phases following stroke. We examined the three most informative components of each inflammatory phase (Fig. 4). The most informative components of the acute phase elastic net model consisted of signalling responses in innate immune cell types (Fig. 4A and Supplementary Table 3). In comparison to the 1-year time point, an increase in pSTAT3 was observed in HLA-DR^{lo} M-MDSCs, $CD14^+CD16^-$ monocytes, and plasmacytoid dendritic cells.

The rapid activation of the transcription factor STAT3 in M-MDSCs, primarily in response to increasing IL-6 plasma concentrations, is a hallmark of the sterile inflammatory response to neurological as well as non-neurological injury (Mayer *et al.*, 2013; Gaudillière *et al.*, 2014). To estimate the effect of stroke on this innate immune response, we compared the pSTAT3 signal in M-MDSCs in samples collected from patients within 1 day after stroke and in samples collected from patients within 1 day after major surgery (Supplementary Fig. 3, the demographics of the surgical patient cohort are summarized in Supplementary Table 1). The results showed comparable pSTAT3 levels in M-MDSCs after stroke and after major surgery.

The most informative components of the intermediate phase model consisted of signalling responses measured in adaptive immune cells (Fig. 4B and Supplementary Table 4). Specifically, pCREB levels were increased at Day 5 after stroke compared to Day 365 in $CD4^+CD25^+FoxP3^+$ T_{regs} and $Tbet^+CD4^+CD45RA^-$ Th1 cells.

The most informative components of the late phase model consisted of a combination of innate and adaptive cell events that differed between Days 90 and 365 (Fig. 4C and Supplementary Table 5). These features included the frequency of neutrophils, pMAPKAPK2 levels in Th1 cells, and pSTAT5 levels in plasmacytoid dendritic cells.

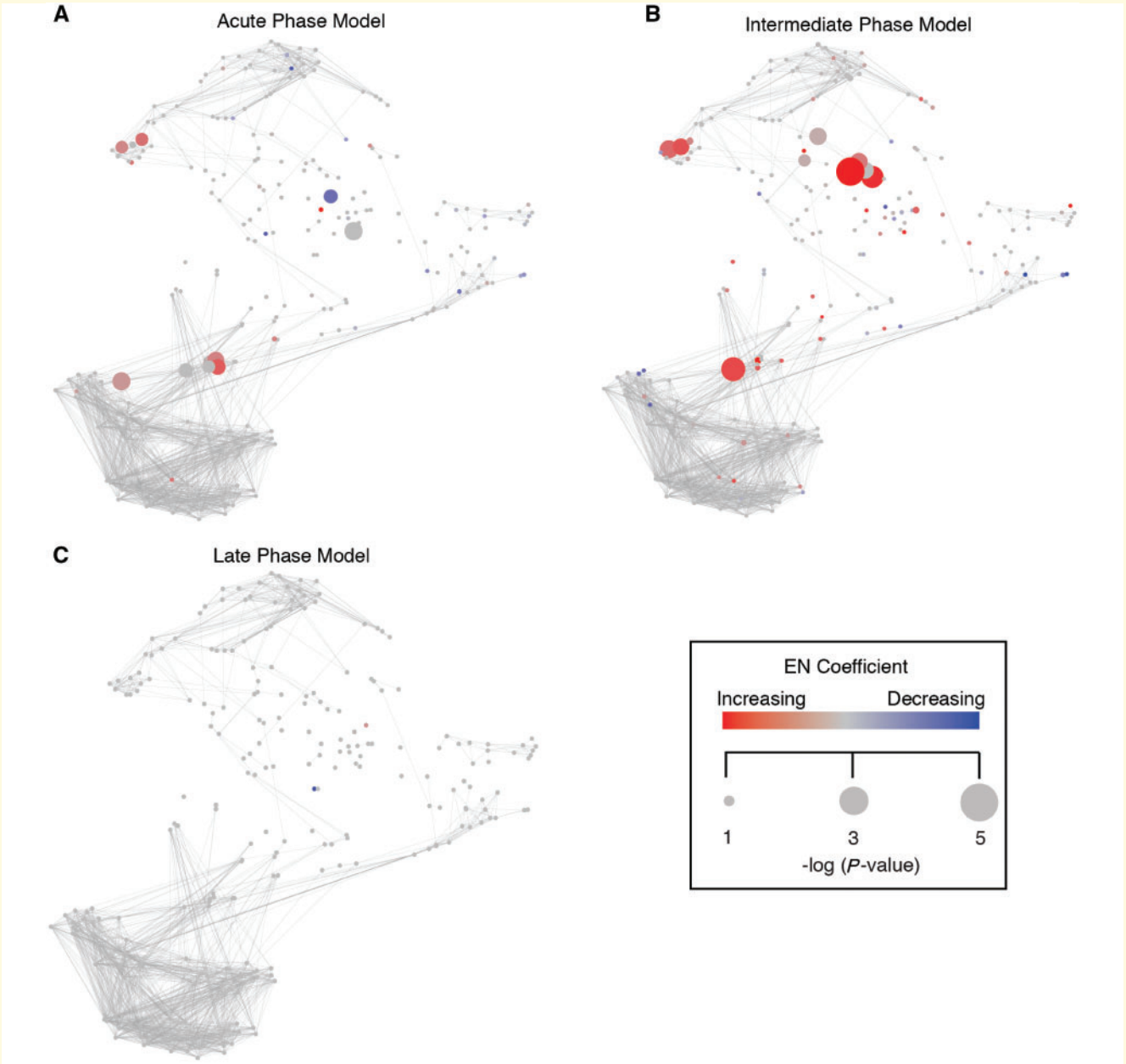

Figure 2 An elastic net analysis identifies three phases characterizing the systemic immune response to acute ischaemic stroke. (**A**–**C**) Comparison of the immunological dataset generated at each time point to the 1-year dataset using elastic net analysis provided three cross-validated elastic net models ($P < 0.01$) that characterized distinct phases of the systemic immune response to stroke. Features selected in the acute (Day 2 versus Day 360, **A**), intermediate (Day 5 versus Day 365, **B**), and late phases (Day 90 versus Day 365, **C**) elastic net models are graphically overlaid on the immune network representing the entire immunological dataset. Red nodes indicate features that are elevated compared to the 1-year time point and blue nodes indicate features that are decreased. Size of node corresponds to the statistical correlation between features and the two time points that make up each model, and intensity of red or blue colour represents the absolute value of elastic net model coefficients at that node. EN = elastic net.

The analysis identified a set of cell-specific immunological events characterizing the peripheral immune state of patients over time after an acute stroke. The magnitude of observed immune responses was surprisingly large. Indeed, it was comparable to immune responses observed in patients undergoing major surgery (Supplementary Fig. 3). However, there was also wide quantitative variability in immune responses among patients after stroke, which prompts the question of whether this variability represents 'background noise' or reflects patient-specific differences that could correlate with differences in stroke severity or outcomes.

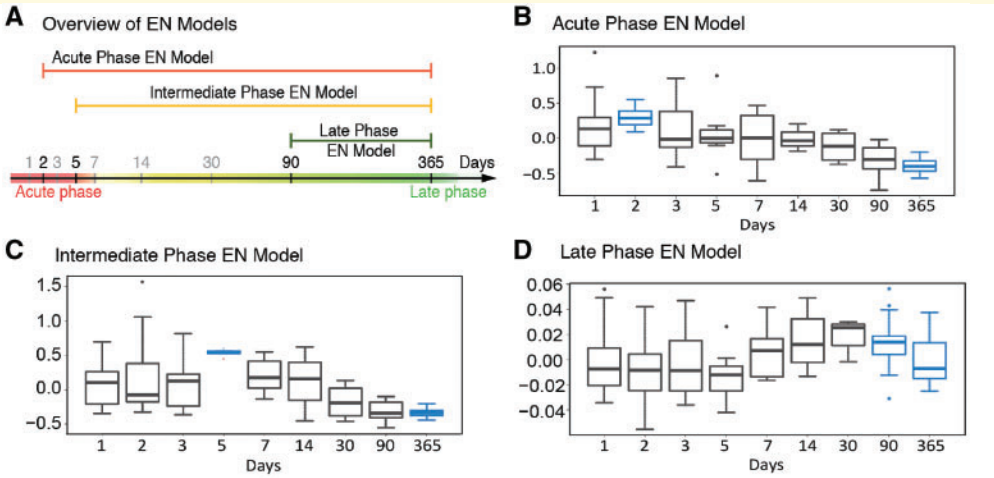

Figure 3 Time-projected elastic net model values reveals the relative magnitude of the acute, intermediate and late inflammatory phase. (**A**) Time span covered by each of the three models. (**B**–**D**) Immune features selected by the acute, intermediate and late elastic net models were quantified at each time point and a time-projected value was inferred for each elastic net model. Box plots depict range of elastic net model values over time, including maximum, minimum, median, and interquartile range, for the (**B**) acute phase model, (**C**) intermediate phase model, and (**D**) late phase model. Time points used to derive each elastic net models are highlighted in blue. EN = elastic net.

The acute phase elastic net model correlates with cognitive trajectories after stroke

To determine the relationship between the multidimensional immunological dataset and patients' cognitive trajectory after stroke, we quantified the change in MoCA scores between Days 90 and 365 after stroke (ΔMoCA). Importantly, cognitive trajectory varied greatly among patients (ΔMoCA, median 0, range −3 to 8, positive changes indicate cognitive improvement; Fig. 5A). Interestingly, ΔMoCA was independent of stroke volume (Fig. 5B). This result is consistent with prior studies showing that stroke size may not be the major determinant of cognitive decline after stroke (Doyle and Buckwalter, 2017).

A correlation analysis was performed between the elastic net model value generated for each model and the ΔMoCA score. A strong negative correlation was observed between the acute phase model values (Day 2) and cognitive trajectory between Days 90 and 365 ($r = -0.692$, Bonferroni-corrected $P = 0.039$, Fig. 5C). This remained significant when accounting for other demographic and clinical variables (including age, sex, BMI, lesion location, and acute treatment modality, Supplementary Table 6). Furthermore, this negative correlation also remained significant and unchanged after controlling for stroke size ($r = -0.664$, $P = 0.026$, Supplementary Table 6), which we identified as a confounding variable correlated with the acute phase elastic net model (Fig. 5D and Supplementary Fig. 4). In contrast, there was no correlation between the intermediate or the late phase models and cognitive trajectory.

Thus, an exacerbated acute inflammatory phase shortly after stroke, primarily defined by elevated pSTAT3 levels in innate immune cell subsets, is associated with worse cognitive outcomes and accounts for over 40% of inter-patient variability.

Discussion

This study used a deep immune profiling approach to characterize the systemic immune response of patients over a period of 1 year following an acute ischaemic stroke. A high-dimensional elastic net analysis of the longitudinal mass cytometry dataset identified three immunological phases that characterized the sequential engagement of innate and adaptive immune compartments after stroke. A strong correlation was observed between immune responses measured during the acute phase (Day 2 after the stroke) and long-term cognitive trajectories. To our knowledge, this is the first report of simultaneously assessed functional and phenotypic attributes of all major immune cell subsets as they occur *in vivo* over a period of 1 year in patients suffering from stroke. The results establish the chronology of peripheral immune cell responses to stroke and provide an analytical framework to identify immunological events associated with adverse clinical outcomes after stroke.

The immune system functions through complex interactions between a broad range of cell types and signalling pathways. Deep profiling of millions of immune system cells in clinical settings has only recently been enabled by high-dimensional mass cytometry. However, computational investigation of the resulting datasets has been limited by two major challenges: (i) the highly interactive nature of the immune system results in a large number of highly correlated measurements; and (ii) the high number of

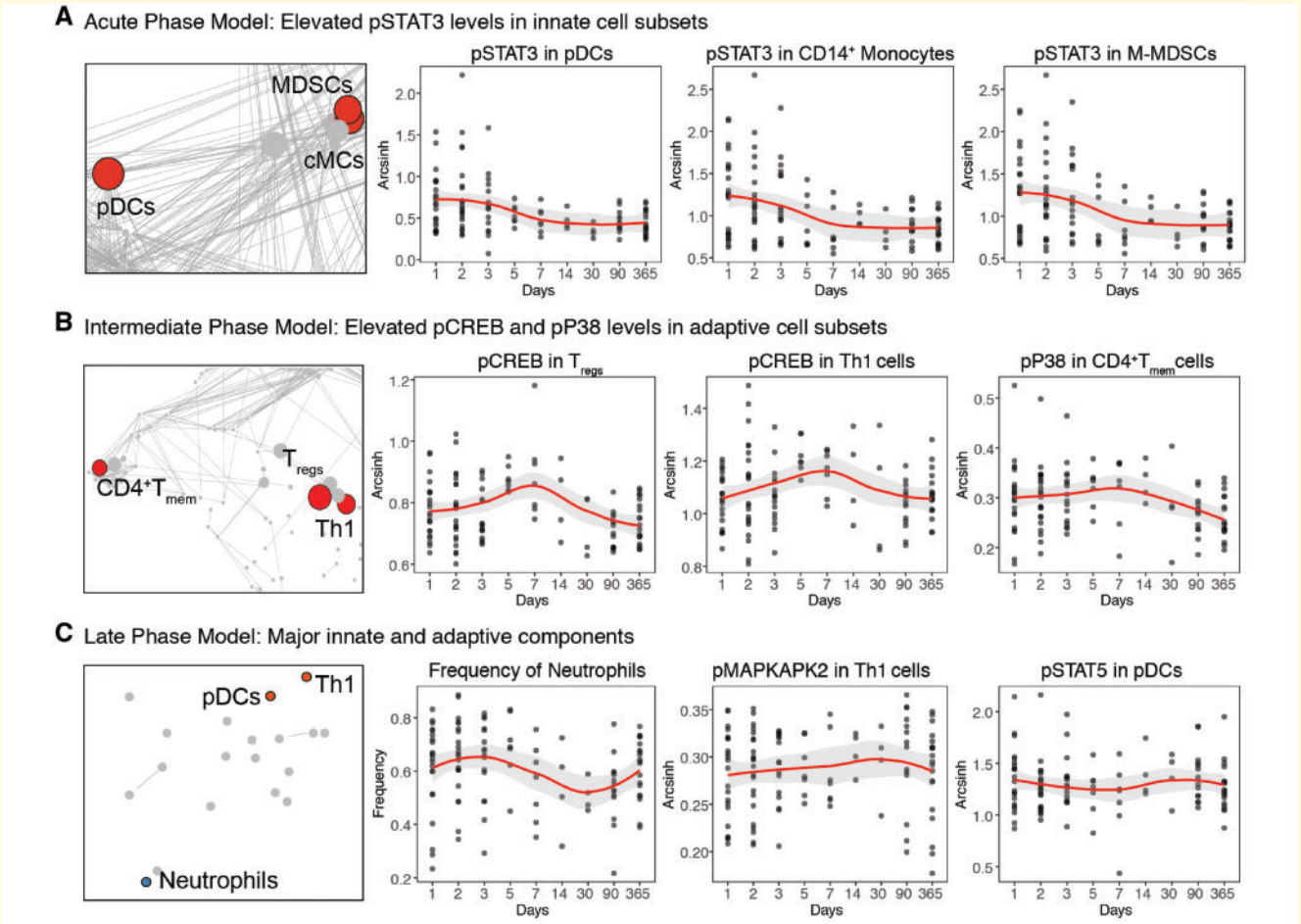

Figure 4 Elastic net components reveal time-specific alterations in innate and adaptive immune responses after acute ischaemic stroke. The components of each elastic net model were nested in communities of highly correlated features that changed concordantly after stroke. The three most significant elastic net components are shown for (**A**) the acute phase model, (**B**) the intermediate phase model, and (**C**) the late phase model. Diagrams on the *left* highlight communities containing the most informative elastic net components. Graphs to the *right* depict the value of elastic net components at each time point (black dots represent individual samples; red lines and grey background represent median and 95% confidence interval, respectively). EN = elastic net; cMCs = classical monocytes; pDCs = plasmacytoid dendritic cells.

measurements and limited sample size is likely to result in a larger number of false-positive discoveries. We addressed both of these challenges using the elastic net analysis, which is a supervised linear model designed to handle datasets with highly inter-correlated features. To ensure generalizability of the results to previously unseen patients, a cross-validation strategy was implemented to report the performance of the models only on patients to which the models where blinded during the training process.

The analysis identified three statistically stringent elastic net models that highlighted acute (Day 2), intermediate (Day 5), and late (Day 90) immunological phases after a stroke. The components of the elastic net models were integrated into communities of correlated immune features that revealed the predominant biological characteristics of each immunological phase. For example, components of the acute phase model demonstrated shared activation of a specific transcriptional event (STAT3 phosphorylation) in multiple innate immune cell subsets. In contrast, components of the intermediate phase model demonstrated coordinated activity of multiple elements of the CREB signalling pathway in adaptive immune cells. In addition, the late phase model identified several sustained immune responses (neutrophil frequency, MAPKAPK2 activity in $Th1_{mem}$ cells, and STAT5 activity in plasmacytoid dendritic cells). Thus, the analysis emphasized entire cellular programs, rather than isolated signalling events, that characterize the chronology of the systemic immune response after stroke. It also identified immunological features that persist for at least 90 days after the stroke event. In combination with late cognitive outcomes, this highlights the value of studying the state of long-term peripheral immune systems in stroke survivors for at least 3 months after stroke.

Aspects of the peripheral immune response observed in this study resonated with prior characterization of immune responses that occur in the brain after stroke

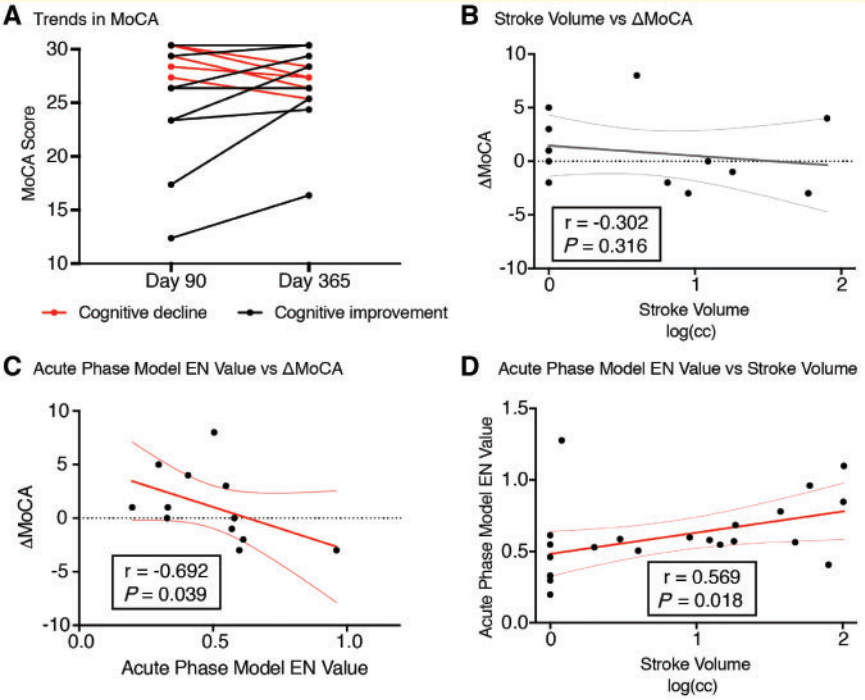

Figure 5 Day 2 immune features comprising the acute phase elastic net model correlate with cognitive trajectories from Days 90 to 365. (**A**) Trajectory of MoCA scores between Days 90 and 365 after stroke. Cognitive stability or improvement is represented by black lines, while cognitive decline is indicated by red lines. (**B**) Stroke volume, measured in log(cm^3), did not correlate with changes in MoCA scores (ΔMoCA). (**C**) Elastic net model values of the acute phase model (Fig. 2A) negatively correlate with ΔMoCA between Days 90 and 365 (Spearman's r = −0.692, Bonferroni-corrected $P = 0.039$). (**D**) Acute phase elastic net values correlated with stroke volume (Spearman's r = 0.569, Bonferroni-corrected $P = 0.018$). EN = elastic net.

(Iadecola and Anrather, 2011). Consistent with the rapid mobilization and recruitment of innate immune cells to the ischaemic site, the acute phase model highlighted the early and robust activation of the STAT3 signalling pathway in innate immune cell subsets. Similarly, the predominance of T cell immune responses (including $CD4^+T_{mem}$, Th1, and T_{reg} cells) in the intermediate phase elastic net model is reminiscent of the delayed engagement of local adaptive and antigen-specific mechanisms after stroke (Doyle and Buckwalter, 2017). These immune cell signalling activities reflect a stereotyped and tightly regulated systemic immune response to stroke that is similar in timing and magnitude to the canonical immune response to tissue injury. In fact, the magnitude of the STAT3 signalling responses of the acute phase elastic net models was remarkably similar to the STAT3 signalling responses observed in patients undergoing major surgery (Supplementary Fig. 3).

Underlying these broad themes, we observed cell-specific immune responses incorporated into each immunological phase that revealed underlying complexity. For example, in the acute phase model, pSTAT3 levels peaked simultaneously in $CD14^+CD16^-$ monocytes, plasmacytoid dendritic cells, and M-MDSCs. This is particularly interesting as STAT3 signalling promotes immunosuppressive functions in MDSCs but, conversely, promotes acute-phase pro-inflammatory responses in monocytes (Levy and Lee, 2002; Vasquez-Dunddel *et al.*, 2013). STAT3 activation drives the differentiation and maturation of plasmacytoid dendritic cells, which has been implicated in autoimmune responses, including in response to endogenous nucleic acids (Swiecki and Colonna, 2015). This example may shed light on simultaneous immune mechanisms that contribute to the peripheral immune response to stroke—it is well known that there is not only an immediate pro-inflammatory response to stroke, but also post-stroke immunosuppression and later auto-immune responses (Dirnagl *et al.*, 2007; Iadecola and Anrather, 2011; Becker, 2012; Chamorro *et al.*, 2012; Doyle and Buckwalter, 2017).

Similarly, key components of the intermediate phase elastic net model included elevated pCREB levels in several T-cell subsets including $CD4^+$ T_{mem}, $Tbet^+CD4^+$ Th1 cells, and T_{regs}. CREB plays a pivotal, but pleiotropic role in T-cell-mediated immune responses and has been proposed to alternately promote or limit the survival and proliferation of T-cell subsets, including Th1, Th2, Th17 and T_{regs} (Wen *et al.*, 2010). The results suggest a dual requirement for CREB in the modulation of pro-inflammatory (Th1-mediated) and anti-inflammatory (T_{reg}-mediated) responses after stroke (Wen *et al.*, 2010). Together, these findings highlight the ability of the immune system to translate similar environmental cues (e.g. elevated plasma levels of JAK2/

STAT3 cytokines, such as IL-6 and IL-10) into cell-specific functional responses implicated in the progression of the ischaemic lesion, as well as in the resolution and recovery after stroke. CREB activity in individual T cell subsets could also be explored in future studies. A comprehensive understanding of which genes CREB is regulating would shed light on the question of how it functionally alters the development or responses of T cells after stroke and whether that promotes or suppresses auto-reactive responses to brain antigens released into the blood after stroke.

The elastic net models captured a chronology of immune events shared among patients following stroke. However, the magnitude of each immunological phase varied greatly among patients. Interestingly, the magnitude of the acute (innate) immunological phase strongly correlated with long-term cognitive trajectories, accounting for over 40% of the observed variance in the change in MoCA scores between the Day 90 and the 1-year time points (ΔMoCA). In contrast, elastic net model values for the intermediate phase, primarily driven by adaptive immune responses, did not correlate with cognitive trajectories. The relative contribution of innate and adaptive immunological events to the pathogenesis of cognitive trajectory after stroke remains poorly understood. Animal studies suggest that cognitive decline after stroke is due to prolonged adaptive immune responses in the brain that are modulated by early innate immune events in the periphery (Doyle *et al.*, 2015). In some stroke survivors, these responses may also account for late declines, such as in cognition and the ability to perform activities of daily living (Ivan *et al.*, 2004; Levine *et al.*, 2015; Corraini *et al.*, 2017; Dhamoon *et al.*, 2017). Our findings in humans are consistent with these preclinical models and suggest that elevated innate immune cell responses within 2 days of a stroke are associated with, and perhaps contribute to, poor cognitive recovery after stroke. However, we did not detect a correlation with the intermediate phase model adaptive immune responses. This may be because of small sample size at intermediate time points, but also could be due to the immunological compartment sampled in our study—it is likely that immune events detected in the peripheral blood do not fully reflect the local events occurring in the brain, particularly at later time points after the blood–brain barrier has begun to be re-established.

Predicting the long-term cognitive trajectory in stroke survivors is a significant clinical challenge. Even after controlling for known risk factors—such as age, sex, common dementia risk factors, stroke volume, and location—having a stroke significantly increases the risk of being diagnosed with cognitive dysfunction over at least the following decade (Ivan *et al.*, 2004; Levine *et al.*, 2015; Corraini *et al.*, 2017). The correlation between the acute phase elastic net model and cognitive recovery remained significant when accounting for demographic (sex, BMI, age) and clinical (CES-D, fatigue scores, NIHSS scores, lesion location, acute treatment modality) variables. Importantly, estimation of the entire acute phase elastic net model at Day 2, rather than measurement of individual components of the elastic net model, was required to detect a strong correlation with patients' long-term cognitive recovery. This result emphasizes the advantage of integrating the functional assessment of multiple immune cell subsets, which act in concert, to identify biological mechanisms associated with a clinically relevant cognitive recovery outcome.

Prior studies have explored immune interventions to improve cognitive function, including two recent studies with natalizumab. Natalizumab blocks alpha 4 integrin on immune cells to prevent their extravasation into tissues. A phase 2 ACTION trial (Elkins *et al.*, 2017) used acute natalizumab (given up to 9 h after stroke) with the aim of reducing infarct size at Day 5, but it failed to meet this primary outcome. However, secondary analyses of two functional scales at 30 and 90 days had mixed results, with improved Rankin at 30 days and improved Barthel Index at 90 days. The follow-up phase 2b study, ACTION2, demonstrated safety in acute stroke patients but was stopped for futility as it was unable to replicate these results. Given our results on change in MoCA from Day 90 to Day 365 we can speculate that natalizumab and other anti-inflammatory treatments given in the acute to subacute window after stroke may affect long-term cognitive outcomes. However, much more remains to be learned from studies of the human peripheral immune response and trials in mouse models of post-stroke dementia before we can do more than speculate on which immunomodulatory agents might be useful in preventing post-stroke dementia. This study is the first step towards understanding how the peripheral immune response is associated with long-term cognitive outcomes.

Our study has limitations. A small cohort ($n = 24$) recruited from a single hospital may not be representative of the entire population of acute ischaemic stroke survivors, which limits the generalizability of the findings. Larger studies involving multiple recruitment centres and more patients will be required to validate our findings. Additionally, a lack of power because of low sampling at some intermediate time points may have resulted in biologically relevant immune changes going undetected. Furthermore, stroke onset is spontaneous so true baseline samples are unobtainable. While we used the Day 365 time point as an internal control for each individual patient, patients may have undergone significant life-style changes including, but not limited to, medications, diet, exercise, and other activities that may have modulated their immune status. Regardless of the cause, variations in the immune response over time between patients may be associated with cognitive outcome.

This study lays the foundation for more comprehensive human studies in the future aimed at targeting specific markers and cell types. It was designed to answer the question of whether stroke-related phenotypical and functional immunological changes could be tracked in peripheral blood

over the course of 1 year. The antibody panel was developed to analyse all major immune components. However, future studies are needed to capture all minor immune cell subsets that may play a role in modulating the immune response, specifically some neutrophil and B-cell subsets. Including intracellular cytokine assays to evaluate additional functional variables in these cell types would also be informative, and stem cell markers could also provide insight into ischaemia-induced multipotent stem cells and their role in neuronal repair following stroke (Tatebayashi *et al.*, 2017). Additionally, the elastic net approach used *a priori*-defined (literature-based) manual gates; another approach is to agnostically cluster immune cells and potentially identify novel cell subsets associated with stroke immune response and recovery.

Our study revealed three immunological phases that represented the systemic immune response of patients during a 1-year recovery period after a stroke. The findings were enabled by high-content, single-cell mass cytometry coupled with an elastic net algorithm that accounts for the dimensionality of the mass cytometry data and the modular structure of the immune system. A strong correlation was observed between the magnitude of the acute immunological phase and long-term cognitive trajectory. Our results were predominantly driven by pSTAT3 levels in innate immune cell subsets measured within 2 days of stroke onset. The analytical framework and timing of cell-specific immune signalling responses that we provide here lays the foundation for future work aimed at determining immune predictors of long-term functional and cognitive trajectories after stroke.

Funding

This work was funded by a 'Big Ideas in Neuroscience' grant from Stanford's Wu Tsai Neurosciences Institute, the Stroke Collaborative Action Network, NIGMS K23 and the Department of Anesthesiology, Perioperative and Pain Medicine at the Stanford School of Medicine.

Competing interests

The authors report no competing interests.

Supplementary material

Supplementary material is available at *Brain* online.

References

Aghaeepour N, Ganio EA, Mcilwain D, Tsai AS, Tingle M, Van Gassen S, et al. An immune clock of human pregnancy. Sci Immunol 2017; 2 (15). pii: eaan2946.

Becker KJ. Activation of immune responses to brain antigens after stroke. J Neurochem 2012; 123: 148–55.

Becker KJ, Kindrick DL, Lester MP, Shea C, Ye Z-C. Sensitization to brain antigens after stroke is augmented by lipopolysaccharide. J Cereb Blood Flow Metab 2005; 25: 1634–44.

Behbehani GK, Thom C, Zunder ER, Finck R, Gaudilliere B, Fragiadakis GK, et al. Transient partial permeabilization with saponin enables cellular barcoding prior to surface marker staining. Cytom Part J Int Soc Anal Cytol 2014; 85: 1011–9.

Bustamante A, Simats A, Vilar-Bergua A, García-Berrocoso T, Montaner J. Blood/brain biomarkers of inflammation after stroke and their association with outcome: from C-reactive protein to damage-associated molecular patterns. Neurotherapeutics 2016; 13: 671–84.

Cella D, Lai J-S, Nowinski CJ, Victorson D, Peterman A, Miller D, et al. Neuro-QOL: brief measures of health-related quality of life for clinical research in neurology. Neurology 2012; 78: 1860–7.

Chamorro Á, Dirnagl U, Urra X, Planas AM. Neuroprotection in acute stroke: targeting excitotoxicity, oxidative and nitrosative stress, and inflammation. Lancet Neurol 2016; 15: 869–81.

Chamorro Á, Meisel A, Planas AM, Urra X, van de Beek D, Veltkamp R. The immunology of acute stroke. Nat Rev Neurol 2012; 8: 401–10.

Corraini P, Henderson VW, Ording AG, Pedersen L, Horváth-Puhó E, Sørensen HT. Long-term risk of dementia among survivors of ischemic or hemorrhagic stroke. Stroke 2017; 48: 180–6.

Dhamoon MS, Longstreth WT, Bartz TM, Kaplan RC, Elkind MSV. Disability trajectories before and after stroke and myocardial infarction: the cardiovascular health study. JAMA Neurol 2017; 74: 1439.

Dirnagl U, Klehmet J, Braun JS, Harms H, Meisel C, Ziemssen T, et al. Stroke-induced immunodepression: experimental evidence and clinical relevance. Stroke 2007; 38: 770–3.

Doyle KP, Buckwalter MS. Does B lymphocyte-mediated autoimmunity contribute to post-stroke dementia? Brain Behav Immun 2017; 64: 1–8.

Doyle KP, Quach LN, Sole M, Axtell RC, Nguyen T-VV, Soler-Llavina GJ, et al. B-Lymphocyte-mediated delayed cognitive impairment following stroke. J Neurosci 2015; 35: 2133–45.

Elkins J, Veltkamp R, Montaner J, Johnston SC, Singhal AB, Becker K, et al. Safety and efficacy of natalizumab in patients with acute ischaemic stroke (ACTION): a randomised, placebo-controlled, double-blind phase 2 trial. Lancet Neurol 2017; 16: 217–26.

Fassbender K, Schmidt R, Schreiner A, Fatar M, Mühlhauser F, Daffertshofer M, et al. Leakage of brain-originated proteins in peripheral blood: temporal profile and diagnostic value in early ischemic stroke. J Neurol Sci 1997; 148: 101–5.

Faul F, Erdfelder E, Lang A-G, Buchner A. G*Power 3: a flexible statistical power analysis program for the social, behavioral, and biomedical sciences. Behav Res Methods 2007; 39: 175–91.

Finck R, Simonds EF, Jager A, Krishnaswamy S, Sachs K, Fantl W, et al. Normalization of mass cytometry data with bead standards. Cytometry A 2013; 83A: 483–94.

Gaudillière B, Fragiadakis GK, Bruggner RV, Nicolau M, Finck R, Tingle M, et al. Clinical recovery from surgery correlates with single-cell immune signatures. Sci Transl Med 2014; 6: 255ra131.

Ghaemi MS, DiGiulio DB, Contrepois K, Callahan B, Ngo TTM, Lee-McMullen B, et al. Multiomics modeling of the immunome, transcriptome, microbiome, proteome and metabolome adaptations during human pregnancy. Bioinformatics 2018; 35: 95–103.

Iadecola C, Anrather J. The immunology of stroke: from mechanisms to translation. Nat Med 2011; 17: 796–808.

Ivan CS, Seshadri S, Beiser A, Au R, Kase CS, Kelly-Hayes M, et al. dementia after stroke: the Framingham Study. Stroke 2004; 35: 1264–8.

Jin R, Yang G, Li G. Inflammatory mechanisms in ischemic stroke: role of inflammatory cells. J Leukoc Biol 2010; 87: 779–89.

Kim JS, Yoon SS, Kim YH, Ryu JS. Serial measurement of interleukin-6, transforming growth factor-β, and S-100 protein in patients with acute stroke. Stroke 1996; 27: 1553.

Konoeda F, Shichita T, Yoshida H, Sugiyama Y, Muto G, Hasegawa E, et al. Therapeutic effect of IL-12/23 and their signaling pathway blockade on brain ischemia model. Biochem Biophys Res Commun 2010; 402: 500–6.

Levine DA, Galecki AT, Langa KM, Unverzagt FW, Kabeto MU, Giordani B, et al. Trajectory of cognitive decline after incident stroke. JAMA 2015; 314: 41.

Levy DE, Lee C. What does Stat3 do? J Clin Invest 2002; 109: 1143–8.

Mayer CA, Brunkhorst R, Niessner M, Pfeilschifter W, Steinmetz H, Foerch C. Blood levels of glial fibrillary acidic protein (GFAP) in patients with neurological diseases. PLoS One 2013; 8: e62101.

Mena H, Cadavid D, Rushing EJ. Human cerebral infarct: a proposed histopathologic classification based on 137 cases. Acta Neuropathol (Berl) 2004; 108: 524–30.

Mrdjen D, Pavlovic A, Hartmann FJ, Schreiner B, Utz SG, Leung BP, et al. High-dimensional single-cell mapping of central nervous system immune cells reveals distinct myeloid subsets in health, aging, and disease. Immunity 2018; 48: 380–95.e6.

Pavlov VA, Chavan SS, Tracey KJ. Molecular and functional neuroscience in immunity. Annu Rev Immunol 2018; 36: 783–812.

Radloff LS. The CES-D scale: a self-report depression scale for research in the general population. Appl Psychol Meas 1977; 1: 385–401.

Shichita T, Ago T, Kamouchi M, Kitazono T, Yoshimura A, Ooboshi H. Novel therapeutic strategies targeting innate immune responses and early inflammation after stroke. J Neurochem 2012; 123: 29–38.

Swiecki M, Colonna M. The multifaceted biology of plasmacytoid dendritic cells. Nat Rev Immunol 2015; 15: 471–85.

Tárnok A. Revisiting the crystal ball - high content single cells analysis as predictor of recovery: editorial. Cytometry A 2015; 87: 97–8.

Tatebayashi K, Tanaka Y, Nakano-Doi A, Sakuma R, Kamachi S, Shirakawa M, et al. Identification of multipotent stem cells in human brain tissue following stroke. Stem Cells Dev 2017; 26: 787–97.

Vasquez-Dunddel D, Pan F, Zeng Q, Gorbounov M, Albesiano E, Fu J, et al. STAT3 regulates arginase-I in myeloid-derived suppressor cells from cancer patients. J Clin Invest 2013; 123: 1580–9.

Waje-Andreassen U, Krakenes J, Ulvestad E, Thomassen L, Myhr K-M, Aarseth J, et al. IL-6: an early marker for outcome in acute ischemic stroke. Acta Neurol Scand 2005; 111: 360–5.

Wang Q, Tang XN, Yenari MA. The inflammatory response in stroke. J Neuroimmunol 2007; 184: 53–68.

Wen AY, Sakamoto KM, Miller LS. The role of the transcription factor CREB in immune function. J Immunol 2010; 185: 6413–9.

Wogsland CE, Greenplate AR, Kolstad A, Myklebust JH, Irish JM, Huse K. Mass cytometry of follicular lymphoma tumors reveals intrinsic heterogeneity in proteins including HLA-DR and a deficit in nonmalignant plasmablast and germinal center B-cell populations. Cytometry B Clin Cytom 2017; 92: 79–87.

Zou H, Hastie T. Regularization and variable selection via the elastic net. J R Stat Soc Ser B Stat Methodol 2005; 67: 301–20.

Zunder ER, Finck R, Behbehani GK, Amir ED, Krishnaswamy S, Gonzalez VD, et al. Palladium-based Mass-Tag Cell Barcoding with a Doublet-Filtering Scheme and Single Cell Deconvolution Algorithm. Nat Protoc 2015; 10: 316–33.